

EMPC: Energy-Minimization Path Construction for data collection and wireless charging in WRSN

Ping Zhong^a, Aikun Xu^a, Shigeng Zhang^{a,*}, Yiming Zhang^b, Yingwen Chen^b

^a School of Computer Science and Engineering, Central South University, Changsha, 410073, China

^b School of Computer, National University of Defense Technology, Changsha, 410073, China

ARTICLE INFO

Article history:

Received 29 September 2020

Received in revised form 3 April 2021

Accepted 12 April 2021

Available online 16 April 2021

Keywords:

Wireless rechargeable sensor network

Data collection

Dual-function vehicle

Energy supplement

Anchor selection

ABSTRACT

Sensing data collection and energy supplement are key issues of Wireless Rechargeable Sensor Network (WRSN). Using mobile vehicles to collect data and supplement energy can not only effectively reduce the node communication energy consumption, but also ensure the continuity of network operation. We propose an energy-minimization path construction algorithm based on dual-function vehicles for data collection and wireless charging in order to minimize the network energy consumption. The algorithm consists of three phases: adaptive network partition, anchor selection, and dual-function vehicle path construction. A partitioning algorithm based on a minimum spanning tree is proposed to divide the network into several regions in the adaptive network partition phase. Anchor selection phase is used to obtain data collection points in each region. The path construction phase is designed to construct a vehicle mobile path with anchors and charging nodes. Finally, experiments show that the algorithm can not only effectively reduce network energy consumption, but also prolong network lifetime and increase collected data amount.

© 2021 Published by Elsevier B.V.

1. Introduction

Wireless rechargeable sensor networks (WRSNs) are composed of a large number of sensor nodes, which can be used for environment monitoring, information transmission, traffic control, and home automation [1]. Efficient data collection is determined by many factors, e.g., battery energy, routing schedules, sensor nodes distribution, and link constraints, which makes sensing data collection one of the key issues in WRSN. Only using a multi-hop static routing method to collect data will increase energy consumption, seriously reduce collected data amount and network lifetime. This method makes the energy problem become an important constraint and challenge to restrict the wide application of sensor nodes.

Recent studies have proposed to utilize mobile vehicles for data collection and wireless charging. For data collection, recent works generally use the combination of single-function data collection vehicles (DCVs) and multi-hop transmission [2–5] to transmit sensing data [6–9]. Some sensor nodes are selected as anchors to collect sensing data within their coverage. DCV moves to each anchor to collect data in the anchors' buffer pool. That not only reduces data collection delay and redundant communication energy consumption caused by the transmission of neighbor node data, but also prolongs network lifetime. Other studies use single-function wireless charging vehicles (WCVs) with wireless energy transfer to solve energy constraints in WRSN. It can provide a more controllable, denser, and sustainable energy supply [10–12]. Thus, the network applies single function vehicles DCV and WCV to collect data and supply energy, respectively.

* Corresponding author.

E-mail address: sgzhang@csu.edu.cn (S. Zhang).

In data collection and energy supplement algorithm based on mobile vehicles, network energy consumption is a key factor to affect network performance such as network lifetime and collected data amount. Compared to energy consumption per unit data collection and energy supplement, the mobile energy consumption per unit of vehicles is larger. Thus, reducing the moving distance of vehicles is a significant way to decrease network energy consumption. When WCV and DCV move to the same sensor node, they will cause double mobile energy consumption, prolong nodes service waiting time, and degrade network performance. Therefore, this paper aims to use dual-function that simultaneous data collection and wireless charging vehicles (DC-WCVs) to complete data collection and energy replenishment [13–15]. To reduce data collection delay and communication energy consumption, some sensor nodes are selected as anchors to collect data in their coverage. DC-WCV moves to each anchor in turn to collect data and supply energy, which makes the network lifetime as long as possible. To avoid sensor nodes death caused by energy exhaustion, DC-WCV can selectively insert some charging nodes into its mobile path. Therefore, this paper aims to design an algorithm for efficient data collection and wireless charging to reduce network energy consumption and increase the collected data amount efficiently.

Considering the constraints of energy, buffer pool, and delay, this paper proposes a DC-WCV mobile path planning problem for energy-consuming devices, sensor nodes, and DC-WCV, to minimize network energy consumption. To solve this problem, an Energy-Minimization Path Construction (EMPC) algorithm is proposed to optimize the network performance. The following itemizes the contributions of this paper.

- Partitioning the network into multiple groups. To ensure the data delay requirements and avoid the overload of anchors in large-scale WRSN, this paper divides the sensors into several regions based on the distance of sensors and the minimum spanning tree length in a region.
- Selecting the anchors for data collection. An anchor selection algorithm based on the node's weight is proposed to construct an appropriate set of anchors, so as to determine nodes must be accessed in a DC-WCV round.
- Constructing an efficient path for DC-WCV. On the premise of satisfying sensor nodes energy, vehicle energy, buffer pool constraints, and data delay requirements, this paper designs an efficient DC-WCV path for anchors and charging nodes to minimize the network energy consumption, extend the network life, and increase the amount of data collected.

The rest of the paper is organized as follows. In Section 2, we present an overview of related work. Section 3 introduces the system model and problem formulation. EMPC algorithm is described in Section 4. Section 5 presents the performance analysis. Finally, we conclude the paper in Section 6.

2. Related work

To collect data and supplement energy efficiently in WRSN, data collection and wireless charging algorithms based on dual-function vehicles have been designed to improve network performance. This section summarizes the work in three aspects related to the scheme proposed in this paper, *i.e.*, network partition [16–18], anchor selection [15,19–23], and mobile path construction [13,24–29].

2.1. Network partition

To reduce energy consumption and data collection delay, a partitioning algorithm based on the minimum spanning tree is proposed in [16]. In this algorithm, internal nodes transmit data to the base station in a multi-hop manner. External nodes collect sensing data by using mobile vehicles. However, the number of WRSN nodes will affect the transmission delay of internal nodes and the state of mobile element that collects data for external nodes. When the number of nodes increases, the mobile element is always busy, and the transmission delay also increases sharply. In social networks with obeying normal distribution, a minimum cut set algorithm based on the normal distribution and a subnet generation algorithm are proposed in [17]. They make subnet and original networks have similar nodes degree distribution, which can greatly reduce the computational complexity. However, this scheme cuts some nodes during the partitioning process and retains the distribution similar to the original network. In contrast, each node in WRSN is very important, so this method is not suitable for the scenario of this paper. A joint mobile data collection and wireless energy transmission strategy responsible for data collection and energy replenishment is proposed in [18]. A Twice-Partition algorithm based on Center Points (TP-CP) is proposed to divide the network into several regions according to the number of mobile vehicles. Different from the TP-CP, our scheme uses the minimum spanning tree to adjust the number of nodes in each partition. The number of nodes in each partition obtained is the same as possible, so that the performance of each DC-WCV can be maximized.

2.2. Anchor selection

Both joint Wireless energy replenishment and anchor-point based Mobile Data Gathering (WerMDG) framework and Anchor Selection algorithm based on Energy of sensor nodes (AS-E) are proposed in [19]. AS-E selects the smallest energy sensor as an anchor to collect sensing data within its coverage area. In [20], a joint charging and data collection model is explored, which follows three-step. Firstly, nodes are divided into clusters. Then, each cluster priority is calculated based

on residual energy and location of nodes. Mobile devices stay in clusters to charge and collect data for nodes. Finally, a scheduling algorithm is used to calculate the minimum number of mobile devices needed to ensure no node death. However, when the sensor nodes are scattered, a large number of clusters will appear in the sensor network. The more clusters, the longer the distance traveled by mobile devices, which is not conducive to the long-term operation of the network. In [15], multiple DC-WCVs are used to collect data and supplement energy for sensors in WRSN. Three anchor selection algorithms are proposed, which are based on the grid algorithm, the Dominating-Set-Based Algorithm (DSBA), and the circular intersection algorithm. Besides, Periodic Energy Replenishment and Data Collection (PERDC) is proposed to maximize network lifetime. In this algorithm, a DC-WCV is allocated to each feasible path through path constraints to schedule a minimum number of mobile devices. A Periodic Multinode Charging and Data Collection (PMCDC) scheme is proposed to keep a perpetual network operation to maximize the amount of data collected by the unit energy of the DC-WCV in [21]. In PMCDC, an anchor point adjustment (APE) strategy is proposed to reduce the sojourn time and the energy consumption of the DC-WCV and further improves the energy utility of the DC-WCV. However, the sensor nodes are scattered, and the number of anchor points is larger, which causes more serious mobile energy consumption in PMCDC. An anchor selection algorithm based on neighborhood node energy is proposed in [22]. Besides, a new mobile device scheduling algorithm is designed to minimize number of mobile devices. However, the importance of node density is ignored in the anchor selection algorithm, which may lead to the increase of the number of anchors, thus increasing the mobile energy consumption of mobile devices. DC-WCVs move to anchors to collect data selected based on the number of neighborhood nodes in [23]. Sensor energy is supplied in the coverage area of DC-WCVs. Compared with other sensor nodes, anchors usually require more energy to maintain normal operation. The remaining energy of the sensor node is not considered when selecting the anchor, which is not reasonable.

2.3. Mobile path construction

In [24], a greedy scheduling algorithm is proposed to maximize network lifetime for periodic energy replenishment and data collection. Robust scheduling is very important to maximize network lifetime for wireless sensor networks [25]. The mobile charger scheduling problem for multi-node recharging with deadline constraints is studied in [26], which aims to maximize the overall effective charging utility and minimize the traveling time for moving as well. In [13], each DC-WCV is responsible for a unique path, which changes with time, effectively reducing data collection delay and node communication energy consumption. However, it takes more energy to fully traverse each sensor node in each tour. In fact, traversing some special nodes (e.g., nodes with high energy consumption) can also meet the requirements of normal network operation. In [27], a novel low-cost code dissemination model is designed based on mobile vehicles with an opportunistic communication style. However, the path construction scheme based on random traversal in WSN is easy to cause the death of nodes due to energy exhaustion. A new network framework is designed for data collection and energy replenishment in rechargeable sensor networks in [28]. It divides DC-WCV mobile path into two types, i.e., charging path and data collection path. To maximize network utility, two paths are exchanged, each of which performs its own duties and does not interfere with each other. Different from our method, this solution divides the mobile path of the DC-WCV into charging path and data collection path. Accessing the same sensor node will require at least double mobile energy consumption. Considering that sensor energy collection is inversely proportional to the square of transmission distance, a remote relay method is proposed in [29]. This algorithm selects node nearer to DC-WCV as an anchor. In remote relay mode, an optimal scheduling strategy is proposed to maximize network utility by combining power allocation, relay selection, and slot scheduling. However, this solution is not friendly to large networks (e.g., networks with a wide distribution area).

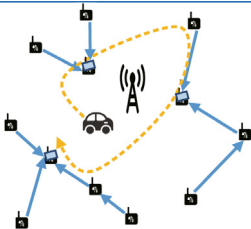
All in all, dual-function vehicles usually complete the process of data collection and energy replenishment through network partition, anchor selection, and mobile path construction. Although some works mention constraints of network devices energy and node buffer pool size, the impact of vehicle battery energy, mobile energy consumption, and dual-function characteristics on the performance of the whole network is not fully taken into account.

3. System model and problem formulation

3.1. Network model

We consider a sensor network consisting N chargeable static sensor nodes, which are randomly deployed in a square sensing area with side length R . Let $S = \{s_1, s_2, s_3, \dots, s_N\}$ be the set of sensors. Each sensor node is equipped with a wireless energy receiving module and battery. If two sensor nodes i and j are in the range of mutual sensing, there is a physical link between node i and j communicating directly. Sensors are monitoring the surrounding environment to obtain data and transmit sensing data to anchors by multi-hop transmission. Then DC-WCV moves to the anchors to collect data and supply energy or moves to the charging node to supply energy. All DC-WCVs are equipped with wireless energy receivers and sensing data receivers.

The network scene diagram is depicted in Fig. 1. The whole network consists of two types of devices: dual-function vehicle DC-WCV that works as a data collector and energy transmitter, sensor nodes that perform to sense the environment. In each round, DC-WCV taking base station as the starting and ending point visits each sensor in turn



Base station



DC-WCV



Anchor



Sensor node



DC-WCV path



Data flow

Table 1
List of notation.

Notation	Definition
N	Set of sensor nodes in the whole network
M	Number of DC-WCVs in the whole network
N^l	Number of sensor nodes in the l th region
L_p	DC-WCV tour length in a round
E_{move}	DC-WCV moving energy consumption in a round
T	A round duration
E_{DATA}^i	Receiving data energy consumption when DC-WCV at sensor i
E_{RF}^i	Supplement energy consumption when DC-WCV at sensor i
T_i	Sojourn time when DC-WCV is at sensor i
f	Data transfer rate from sensor to DC-WCV
η	Energy transfer rate of DC-WCV
P_i	Energy consumption per second of sensor i
E_{node}	Sensor battery energy
E_{DC-WCV}	DC-WCV battery energy
b	Buffer pool of sensor
D	Sensing data delay constraint of sensor
L_{MST}^l	Minimum spanning tree length of partition l
L_{avg_MST}	Average spanning tree length

(a) *Mobile energy consumption.* L means DC-WCV cycle path passing through the set $n = \{n_1, n_2, n_3, \dots, n_{|n|}\}$. L_{min} means the shortest Hamiltonian cycle passing through the set n . L_{max} means the valid path with maximal length passing through the set n , where $L_{max} = \sqrt{2(|n| - 2)ab} + 2(a + b)$ [31,32]. a and b represent the length and width of the rectangular area when the region is covered by a rectangle. L_p means constructed path length of cycle path L . $d_{i,i+1}$ represents the length of edge (n_i, n_{i+1}) in set L . DC-WCV moving path length constraints can be expressed as

$$L_{min} \leq L_p = \sum_{i=1}^{|n|} d_{i,(i+1),mod|n|} \leq L_{max}. \quad (4)$$

The mobile energy consumption of DC-WCV in a round is

$$E_{move} = L_p e_{move}, \quad (5)$$

where e_{move} means unit mobile energy consumption of DC-WCV.

(b) *Receiving sensing data energy consumption at the anchor.* We assume that the data sensing rates of all rechargeable sensor nodes obey Poisson distribution with mean value λ [32]. The maximum data sensing of a node is $F_{\lambda}^{-1}(\varepsilon)$. Because of $F_{\lambda}^{-1}(1) \rightarrow \infty$, ε is a value close to but not equal to 1. $\varepsilon = 0.99$ based on [32]. The maximum collected data amount by DC-WCV from node i and the required energy are expressed respectively as

$$DATA_i = F_{\lambda}^{-1}(\varepsilon)|A_i|, \quad (6)$$

$$E_{DATA}^i = F_{\lambda}^{-1}(\varepsilon)|A_i|E_r, \quad (7)$$

where $|A_i|$ represents the number of nodes contained in the tree rooted by sensor node i . E_r means energy output in the receive circuit, which is a fixed parameter.

(c) *Supplementing energy consumption for sensor nodes.* DC-WCV can provide radio frequency energy for sensor nodes while visiting sensors. According to the type of visiting nodes, DC-WCV's service sensors can be divided into radiofrequency energy for anchors and radiofrequency energy for charging nodes.

Radiofrequency energy for anchors. The time receiving sensing data at anchor is usually longer than its supplementary energy time. To ensure the effectiveness of sensing data, the sojourn time at each anchor is equal to the time spent on receiving perceptual data. Based on collected data amount at sensor i , the sojourn time at sensor i is

$$T_i = DATA_i / f, \quad (8)$$

where f is the data transmission rate from the sensor to DC-WCV. When DC-WCV stays at the sensor node i , radiofrequency energy supplement by DC-WCV for sensor i is

$$E_{RF}^i = T_i e_{RF} \eta, \quad (9)$$

where e_{RF} is an energy transfer rate from DC-WCV to a sensor, which unit is J/s. η is the energy transfer efficiency of DC-WCV.

Radiofrequency energy for charging nodes. When the sensor battery energy is lower than a certain value, DC-WCV will receive the charging request sent by the sensor. Then DC-WCV will insert the charging node into its service queue and move to the node for wireless charging. Let t_1 be the sending time of charging request, t_2 be the arriving time of DC-WCV moving to the charging node. Energy consumption by the charging node in this period is

$$E_{wait}^i = (t_2 - t_1)P_i, \quad (10)$$

where P_i denotes the unit energy consumption of sensor i in J/s, which can be expressed as

$$P_i = E_s * r_i + \sum_{c \in Children(i)} E_r * r_c + (r_i + \sum_{c \in Children(i)} r_c) * (E_t + \varepsilon d_{ij}^2), \quad (11)$$

where r_i means data sensing rate for sensor i in bit/s. $Children(i)$ denotes a set of children nodes of sensor i . $c \in Children(i)$ means sensor c is a child of sensor i . $Parent(i)$ denotes a set of parent nodes of sensor i . d_{ij} represents the distance between sensor i and sensor j . Eq. (11) means the unit energy consumption of sensor i . It consists of data sensing energy consumption, receiving energy consumption, and transmission energy consumption to the parent node.

To ensure sensing data effectiveness and replenishing charging nodes' energy in time, DC-WCV leaves charging nodes and serves the next node while replenishing node battery to a certain value. Thus, charging threshold of the sensor i (i.e., $E_{threshold}^i$) is not more than the node battery capacity E_{node} . $E_{threshold}^i$ is not less than charging request threshold E_{req}^i , where $E_{req}^i \leq E_{threshold}^i \leq E_{node}$. Because of different energy consumption per unit of each sensor node, the charging request threshold is setting based on the sensor's remaining time. When the residual time of node t is less than d_{max}/v , namely $E_{req}^i \leq tP_i$, the node immediately sends a charging request to DC-WCV. d_{max} means distance between the farthest two nodes in a region. The charging threshold ensures that each charging node has sufficient time to replenish energy. The charging threshold of sensor i can be expressed as

$$E_{threshold}^i = (E_{node} - E_{req})\sqrt{N^l - L'/N^l} + E_{req}^i, \quad (12)$$

where L' denotes the number of un-served nodes in the current DC-WCV queue. Eq. (12) shows that there is a negative correlation between L' and $E_{threshold}^i$. When L' is larger, the corresponding $E_{threshold}^i$ is smaller. It ensures that charging nodes can be serviced in time. Based on the charging request threshold and charging threshold, radiofrequency energy supplemented by DC-WCV for sensor i is

$$E_{serve}^i = E_{threshold}^i - E_{req}^i. \quad (13)$$

When the number of DC-WCV service nodes is $|n|$, energy supplemented by DC-WCV for anchors is $\sum_{i=1}^{|A|} T_i e_{RF} \eta$. Besides, energy supplemented by DC-WCV for charging nodes is $\sum_{j=1}^{|n|-|A|} E_{serve}^j$ based on (13).

Based on DC-WCV mobile path length, sojourn time at sensor i , and energy supplement for charging nodes, a round duration is expressed as

$$T = L_p/v + \sum_{i=1}^{|A|} T_i + \sum_{j=1}^{|n|-|A|} E_{serve}^j / e_{RF} \eta, \quad (14)$$

where v is the speed of DC-WCV. When $|n| = |A|$, it means DC-WCV service nodes only include anchors, and the time consumed at charging nodes is zero. When the number of DC-WCV service nodes is $|n|$ in a round, the energy consumption minimization problem of DC-WCV can be expressed as

$$\min E_{move} + \sum_{i=1}^{|A|} E_{DATA}^i + \sum_{i=1}^{|A|} \frac{E_{RF}^i}{\eta} + \sum_{j=1}^{|n|-|A|} \frac{E_{serve}^j}{\eta}. \quad (15)$$

3.3.2. Sensor

Sensors' energy is mainly used for sensing and transmitting data. Based on a round duration T , the energy consumption minimization problem of sensors can be expressed as

$$\min \sum_{i=1}^{N^l} TP_i. \quad (16)$$

x_{ij} is a binary decision variable, which means whether $arc(i, j)$ is on DC-WCV path. When $arc(i, j)$ is on DC-WCV path, $x_{ij} = 1$ and $i, j \in N^l$; otherwise $x_{ij} = 0$. x_{ij} is

$$x_{ij} = \begin{cases} 1, & \text{arc}(i, j) \text{ is on DC-WCV path} \\ 0, & \text{Other wise} \end{cases}. \quad (17)$$

Based on the above energy consumption analysis, the minimizing network energy consumption problem can be transformed into the following non-linear optimization problem.

$$\min E_{move} + \sum_{i=1}^{|A|} E_{DATA}^i + \sum_{i=1}^{|A|} \frac{E_{RF}^i}{\eta} + \sum_{j=1}^{|n|-|A|} \frac{E_{serve}^j}{\eta} + \sum_{i=1}^{N^l} TP_i, \quad (18)$$

Subjected to

$$L_{min} \leq L_p \leq L_{max}, \quad (19)$$

$$\sum_{j=2}^{N^l} x_{1j} = 1, \quad (20)$$

$$\sum_{j=2}^{N^l} x_{j1} = 1, \quad (21)$$

$$F_{\lambda}^{-1}(\varepsilon) \geq r_i, i \in N^l, \quad (22)$$

$$F_{\lambda}^{-1}(\varepsilon)|A_i|T \leq b, \quad (23)$$

$$f_i^{out} = \left(\sum_{c \in \text{Children}(i)} f_c^{in} \right) + r_i, \quad (24)$$

$$TP_i \leq E'_i + E_{serve}^i, \quad (25)$$

$$E_{move} + \sum_{i=1}^{|A|} E_{DATA}^i + \sum_{i=1}^{|A|} \frac{E_{RF}^i}{\eta} + \sum_{j=1}^{|n|-|A|} \frac{E_{serve}^j}{\eta} \leq E_{DC-WCV}, \quad (26)$$

$$T \leq D, \quad (27)$$

where $\forall i, c \in N^l$. b means the size of the node buffer. f_i^{out} represents the output data flow of sensor i . f_i^{in} represents the input data flow of sensor i . D denotes sensing data delay constraints. E'_i is the residual energy of sensor i .

The optimization objective function, as shown in (18), represents the total energy consumption of dual-function vehicles and sensors in a round. Eq. (18) indicates energy consumed by DC-WCV for moving, receiving anchors data, supplying energy and sensors respectively in a round. Considering battery energy constraints, buffer pool constraints, and perceived data delay constraints, this paper aims to plan and design an efficient DC-WCV mobile path to minimize the total energy consumption.

These constraints can be explained as follows. Eq. (19) denotes DC-WCV moving path is a feasible and a connected loop. Eq. (20) ensures DC-WCV starts from the base station in a round. Eq. (21) ensures DC-WCV eventually returns to the base station in a round. Here, 1 represents the network base station. Eq. (22) indicates that data sensing rate obeying Poisson distribution is always less than the maximum data sensing rate. $F_{\lambda}^{-1}(\varepsilon)$ means the maximum data sensing rate. Eq. (23) means data amount in sensor buffer is less than the sensor buffer pool size to avoid overflow phenomenon in the worst case. T means a round duration. Eq. (24) denotes the data flow constraints of sensor nodes. The output flow is equal to input data of its sub-nodes and its own sensing data flow. The constraint Eqs. (25)–(26) are battery energy constraints of sensors and DC-WCV. Eq. (25) means the total energy consumption of the sensor is less than the sum of its own energy and supplementary energy. Eq. (26) guarantees DC-WCV energy consumption for moving, receiving data, and energy supplement never exceeds total energy, which ensure the vehicle can always return to the base station to replenish energy. Eq. (27) means data delay constraints, which indicates a round duration is less than data delay to ensure data effectiveness.

4. The proposed EMPC algorithm

An Energy-Minimization Path Construction (EMPC) algorithm is proposed to solve the objective function (18) by designing DC-WCV mobile path satisfying (19)–(27). Firstly, the EMPC algorithm divides a WRSN into several regions and deploys a DC-WCV for data collection and energy supply in each region. Then, some sensors are selected as anchors to collect data. Next, the EMPC algorithm optimizes an efficient DC-WCV mobile path for sensors to minimize network energy consumption. Finally, DC-WCV replenishes energy and/or collects data for sensors according to its mobile path. EMPC algorithm is introduced in detail as follows.

Fig. 2 shows the process of EMPC. The rectangle area indicates the sensing area. Red pentagon at the center means base station. The blue dotted line divides the sensing area into four regions in Fig. 2(a). There is a minimizing spanning tree rooting at the base station in each region. In Fig. 2(b), some sensors are selected as anchors to collect data within its area, which are represented by a solid diamond. Data transmission routing from the sensor to anchor is represented by the black solid line. In Fig. 2(c), DC-WCVs' tour paths are constructed by a gray dotted line. They consist of anchors and charging nodes. On the one hand, the DC-WCVs move to the charging node and provide energy for it. On the other hand, the DC-WCVs move to the anchor to collect its data and supply energy for it.

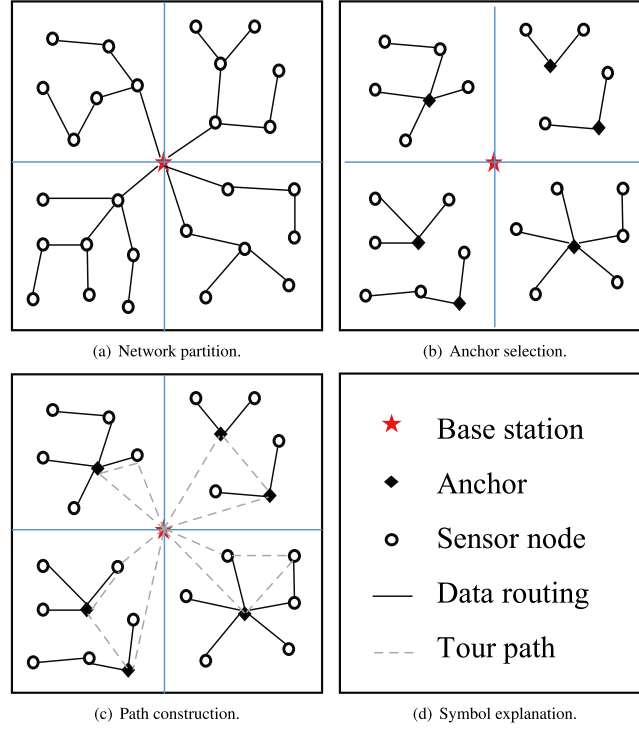


Fig. 2. The process of EMPC.

4.1. Adaptive network partition

An adaptive Network Partition algorithm based on Minimum Spanning Tree (NP-MST) is proposed, which first chooses M center points as the basis of the initial network partition. To ensure that selected M center points are dispersed and not centralization, the whole network is divided into M regions according to sensing area shape and base station orientation. Each region is covered by a rectangle. Then, center points are selected based on the minimum sum of the linear distances of other sensor nodes in each region. In the l th region, the sum of the distances from sensor i to other nodes is expressed as

$$S_i = \sum_{j=1}^{N^l} d_{ij}, \forall j \in N^l. \quad (28)$$

Then, the sensor with the smallest S_i in each region is selected as the initial center point. Besides, the shortest routing hop from the sensor to center points is the criterion of a network partition. The shortest routing hops set from sensor i to M center points are calculated, $H = \{h_i^1, h_i^2, \dots, h_i^M\}$ and $\forall i \in N$. The minimum h_i^l means sensor i will be assigned into the l th region, where $1 \leq l \leq M$. Repeat this process until all sensors are assigned. Then the center points are recalculated based on (28) in the new region. The whole network is repartitioned according to the shortest routing hop from the sensor to center points. Repeat the network partition process until the center points result does not change.

There may be a large difference in the number of sensors between different regions after dividing the network. The minimum spanning tree is used to adjust each region's nodes. The adjustment process is divided into two steps. The adaptive network partition algorithm is shown in Algorithm 1.

Tree length calculation. The minimum spanning tree based on the base station (i.e., root node) is constructed in each partition. Calculate the minimum spanning tree length L_{MST}^l , where $1 \leq l \leq M$. The average spanning tree length $L_{avg_MST} = \sum_{l=1}^M L_{MST}^l / M$ is calculated based on L_{MST}^l .

Node adjustment. The absolute value of the difference between L_{MST}^l and L_{avg_MST} is compared in turn. If all absolute values are not greater than the constant of D_value , the partition ends. Otherwise, nodes with larger spanning tree length will be divided into an adjacent partition with smaller spanning tree length. The principle of division is as follows. A line segment has two endpoints. One is the base station. The other is any node in partition 1. Keep the endpoint of the based station fixed and rotate the line segment. Divide a node that the line segment first meets in partition 2 into partition 1. After traversing all regions, recalculate L_{MST}^l and L_{avg_MST} . Repeated until the absolute value of the difference between L_{MST}^l in each partition and L_{avg_MST} is not greater than D_value .

Algorithm 1 NP-MST

Input: N sensor nodes, M DC-WCVs, center point list C .
Output: region N^l .

- 1: Divide the network into M regions equally, denote nodes in the l^{th} region as N^l .
- 2: Initialize part index $m = 1$, center point list copy $C_1 = \emptyset$.
- 3: **while** m is smaller than M **do**
- 4: $N^{l1} = N^l$;
- 5: **while** N^{l1} is not exhausted **do**
- 6: $S_i = \sum_{j=1}^{N^l} d_{ij}$, Remove node i in N^{l1} ;
- 7: **end while**
- 8: Select $\min\{S_i, i \in N^l\}$ and insert node i into C ;
- 9: **end while**
- 10: **while** $C_1 \neq C$ **do**
- 11: $N1 = N$;
- 12: **while** $N1$ is not exhausted **do**
- 13: $H = \{h_i^1, h_i^2, \dots, h_i^M\}$;
- 14: Remove node i in $N1$;
- 15: h_i^M means shortest routing hop between node i to center point M ;
- 16: Select $\min\{h_i^l, \forall i \in N\}$, assign the node i into l^{th} region;
- 17: **end while**
- 18: Recompute the center point S_i in each region, and insert node i into C_1 ; $C = C_1$; $C_1 = \emptyset$;
- 19: **end while**
- 20: Compute minimum spanning tree length in each region L_{MST}^l , where $1 \leq l \leq M$;
- 21: Compute average spanning tree length L_{avg_MST} ;
- 22: $L_{avg_MST} = \sum_{i=1}^l L_{MST}^l / M$;
- 23: **while** $L_{MST}^l - L_{avg_MST} > D_value$ **do**
- 24: $m = 1$;
- 25: **for** m is smaller than M **do**
- 26: Contrast the L_{MST}^m of adjacent partition in turn;
- 27: Put node i in partition with higher L_{MST}^m into the partition with lower L_{MST}^m ;
- 28: Recompute the L_{MST}^m ;
- 29: **end for**
- 30: Recompute the L_{avg_MST} ;
- 31: **end while**

Fig. 3 shows the network partition result of NP-MST. 100 rechargeable sensor nodes are randomly distributed in a square area of $100 \text{ m} \times 100 \text{ m}$. Sensing range of each node is $d_r = 15 \text{ m}$. The red pentagon at the center of the sensing area represents the base station. Sensor nodes are represented by four icons (cross character, hollow circle, asterisk, and cross sign) after network partition. Fig. 3(a) shows the result of the equalization network. Fig. 3(b) show the results of partitioning networks based on the shortest routing hops. Fig. 3(c) shows the result of partitioning the network based on the minimum spanning tree. The number and distribution of sensors in Fig. 3(b) and (c) are different from those in Fig. 3(a). The number of nodes in a single area is significantly different. Due to the same hardware configuration of DC-WCVs, unbalanced network partition may lead to a long idle period of DC-WCV in the region with fewer sensor nodes. However, the DC-WCV is always busy in the region with more nodes. After adjusting the network based on the minimum spanning tree, the number of sensor nodes in each region of Fig. 3(c) is more uniform. The green dotted line represents nodes divide changed areas compared with the previous picture. Fig. 4 shows the minimum spanning tree comparison before and after adjustment. Fig. 4(a) shows the minimum spanning tree in each partition before adjustment. Fig. 4(b) shows the minimum spanning tree in each partition after adjustment.

4.2. Anchor selection

Some sensors are chosen as anchors with high battery energy and good sociability to collect sensing data within the coverage area. Therefore, an Anchor Selection algorithm based on the Density and Energy of sensor nodes (AS-DE) is proposed to select some nodes as anchors.

Matrix X indicates whether any two nodes i and j are connected within k hops. Matrix X as

$$X_{ij} = \begin{cases} 1, & i \text{ and } j \text{ are connected in } k \text{ hops} \\ 0, & i \text{ and } j \text{ are not connected in } k \text{ hops or } i = j \end{cases} \quad (29)$$

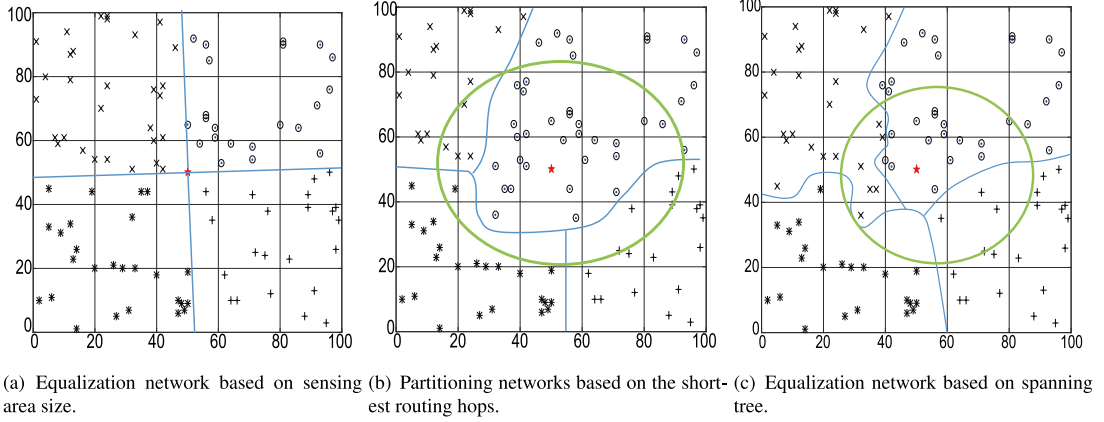


Fig. 3. An adaptive network partition example of NT-MST.

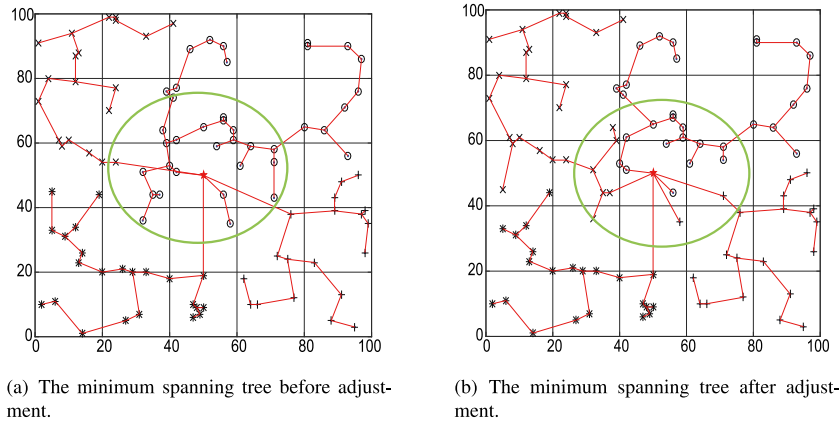


Fig. 4. The minimum spanning tree comparison before and after adjustment.

Sensor density refers to the ratio of the total number of nodes within k hops to the total number of nodes in a partition. The density of sensor i can be expressed as

$$\rho_i = \left| \sum_{x=1}^k N_{x,hop}(i) \right| / N^l, \quad (30)$$

where $N_{x,hop}(i)$ means neighborhood node-set in the x hop of sensor i , where $\left| \sum_{x=1}^k N_{x,hop}(i) \right| = \sum X_i$. Weights of sensor node i considering battery energy and sociability as

$$W_i = \alpha \rho_i + (1 - \alpha) E_i / E_0, \quad (31)$$

$$E_0 = \min\{E_j | X_{ij} = 1\}, \quad (32)$$

where E_0 denotes the minimum battery energy of node i in k hop neighborhood set. E_i means residual energy of node i . α represents importance, where $0 \leq \alpha \leq 1$.

Sensors are sorted from high to low in a partition based on sensor weight. Node with the largest weights is selected as an anchor, which is added to anchor set A . Then remove the nodes within the anchor k hop neighborhood. Reselect node with the largest weights. Repeat the process until each node in the partition has a unique anchor and satisfies the constraint (19). If TSP path of anchors and base station is less than path threshold L_b , a non-anchor node with the largest weights is chosen to add to anchor set A . Repeat anchor addition process until the TSP is just less than L_b and satisfies the constraint (19). The anchor selection algorithm is shown in Algorithm 2.

Anchor selection is closely related to variable k , which can affect the data transmission path and sensors' energy consumption. Therefore, k is set to 2 based on Ref. [32]. 100 rechargeable sensor nodes are randomly distributed in a $100 \text{ m} \times 100 \text{ m}$ square network. Fig. 5 shows an example of an anchor selection result based on AS-DE. Blue solid points represent anchors. Black dotted lines represent TSP paths constructed by anchors and base stations. The four TSP paths represent the shortest paths composed of anchors and base stations in four regions respectively.

Algorithm 2 AS-DE**Input:** sensor nodes N^l in a region, connected matrix X .**Output:** anchor point list A .

```

1:  $N^{l1} = N^l$ ;
2: while  $N^{l1}$  is not exhausted do
3:   Compute node density  $\rho_i$ ;
4:    $\rho_i = |\sum_{x=1}^k N_{x\_hop}(i)|/N^l$ ;
5:   Compute  $W_i = \alpha \rho_i + (1 - \alpha)E_i/E_0$ ;
6:    $0 \leq \alpha \leq 1$ ;
7:   where  $E_0 = \min\{E_j | X_{ij} = 1\}$  and  $E_i$  is node  $i$  battery;
8:   Sort  $\{W_i\}$  in an increasing order;
9:   Remove node  $i$  in  $N1$ ;
10: end while

```

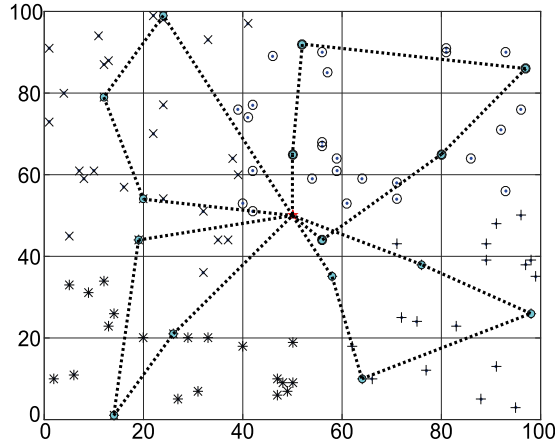
**Fig. 5.** An example of anchor selection.

Fig. 6 shows an example of data transmission in each partition. Solid blue dots are anchors for each partition. The red solid line represents the sensing data transmission link. We can see that each sensor with multiple or zero child nodes has a unique parent node. The data transmission link, anchor, and its members can be regarded as a data transmission tree. The anchor is seen as the root and members are seen as descendant nodes.

4.3. Path construction

Set $L = \{l_m | 1 \leq m \leq N_l\}$ denotes DC-WCV service queue. All anchors are included in set L . There may be charging nodes in L , if DC-WCV receives charging requests. This paper aims to minimize network energy consumption by constructing mobile vehicle paths. The vehicle path construction process is divided into anchor path construction and charging node insertion.

4.3.1. Anchor path construction

Anchor path construction process consists of two steps. Firstly, a convex polygon is constructed by using some anchors. Secondly, remaining anchors are inserted into the convex polygon. When any side of a polygon extends infinitely into a straight line, the other edges are on one side of the line. This polygon is called a convex polygon. Set $L' = \{l_0, l_1, l_2, \dots, l_{|A|}\}$ means residence points of vehicle in a region, where l_0 is the base station and $|A|$ is anchors number. The convex polygon is constructed with l_0 as a starting and endpoint [33]. Polygon vertices set is $\{l_0, l_1, l_2, \dots, l_c\}$. $c < |A|$ means remaining $(|A| - c)$ anchors are not included in polygon vertices set. Let set $L'' = \{l_{c+1}, l_{c+2}, \dots, l_{|A|-1}, l_{|A|}\}$ denotes remaining anchors. Then, based on The Triangle Inequality Theorem (i.e., The sum of any two sides of a triangle must be greater than the measure of the third side), the remaining anchors are inserted into the convex polygon to construct the shortest path of all anchors. Let $d(l_x, l_y)$ denote distance between l_x and l_y . l_{cl} is the anchor to be inserted into the convex polygon and $l_{cl} \in L''$. $D_{increment}(l_x, l_y)$ represents movement increment that inserting an anchor l_{cl} to adjacent points l_x and l_y in *Path*. It can be expressed as

$$D_{increment}(l_x, l_y) = d(l_x, l_{cl}) + d(l_{cl}, l_y) - d(l_x, l_y). \quad (33)$$

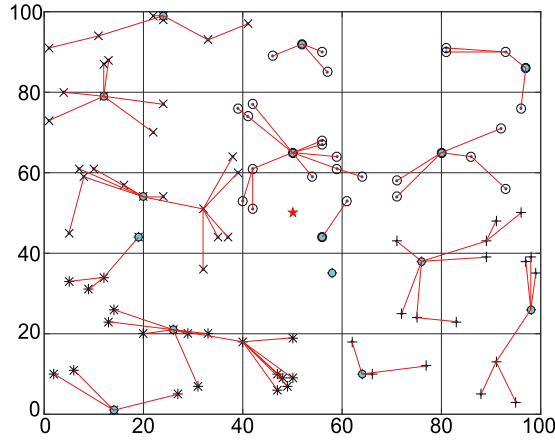


Fig. 6. Data transmission example diagram.

Select the minimum $D_{\text{increment}}(l_x, l_y)$ while l_{cl} is inserted into two adjacent points l_x and l_y in $Path$ in turn. Delete anchor l_{cl} in remaining anchors set L'' . And rearrange node number in $Path$. Repeat the process until the set L'' is empty. A vehicle moving path is $Path = (l_0, l_1, l_2, \dots, l_{|A|}, l_0)$. The convex polygon scheme guarantees that only one tour can be constructed and no extra distance will be added. The Triangle Inequality Theorem is the theoretical support of the movement increment. The anchor with the minimum movement increment is inserted between the other two anchors to ensure that the total path of the new tour is always minimal. The above two advantages ensure that the tour constructed by the anchor path construction method is minimal.

4.3.2. Charging node insertion

The vehicle may receive charging requests at any time and only serves the next node in $Path$ after serving the current one. $ChargingReq$ means charging request queue of charging node. Charging node will be inserted into $ChargingReq$ once the vehicle receives a charging request. When the vehicle leaves the current service node and chooses the next node in $Path$, it first checks whether $ChargingReq$ is empty. If $ChargingReq$ is empty, vehicle directly chooses the next node in $Path$. Otherwise, charging nodes in $ChargingReq$ are ranked according to the remaining time of nodes. Node with the minimum remaining time is marked as 1. Then charging nodes are ranked based on the distance between the vehicle and charging nodes. Node with the minimum distance is marked as 1. On this basis, charging nodes are arranged in ascending order according to sum of remaining time rank and distance rank. Besides, the first node i in $ChargingReq$ is inserted into $Path$ based on (33) and judge whether the constraints (19)–(27) is satisfied. If it is satisfied, the node is inserted into $Path$ and $ChargingReq = ChargingReq - i$. Otherwise, traverse the next node in $ChargingReq$ until $ChargingReq$ traverses once. Finally, the vehicle serves the next node based on the new $Path$.

Fig. 7 shows path construction process of DC-WCV. Fig. 7(a) shows DC-WCV mobile path $Path = (l_0, l_1, l_2, \dots, l_{10}, l_0)$ composed of 10 anchors and base stations, where l_0 represents base station. Fig. 7(b) indicates that when DC-WCV moves to l_1 , it receives charging requests from C_1, C_2, C_3, C_4 . This paper assumes that charging node C_1 is inserted into DC-WCV mobile path. Feasibility of inserting C_1 is judged by the optimization function constraints. Fig. 7(c) shows that optimization function constraints are satisfied when charging nodes C_1, C_2, C_3 are inserted into $Path$. TSP algorithm is used to construct the shortest mobile path of charging node, anchors, and base station. Fig. 7(d) shows the re-numbering of service nodes in DC-WCV $Path$. It is expressed as $Path = (l_0, l_1, l_2, \dots, l_{13}, l_0)$, where l_0 is the starting point of $Path$.

5. Performance evaluation

We use a PC with 64 Intel(R) Core(TM) i7-4790 CPU 3.60 GHz, 8G memory, 1TB disk, and Matlab2016a for simulation. We assume that the WRSN consisting of 100 sensors, a base station, and four dual-function vehicles DC-WCVs. Sensors are randomly distributed in a square area of 100 m \times 100 m. The base station is at the center of the sensing area. The connection between two nodes indicates that two nodes can wirelessly communicate with each other. All sensor nodes have the same hardware configuration and wireless transceiver module. Sensors data sensing rate obeys Poisson distribution with $\lambda = 3$ B/s. The initial energy of sensors is 50 J and the communication range is 15 m. Single hop transmission delay is 1 s. Other parameters setting are $f = 50$ B/s, $\eta = 30\%$, $v = 3$ m/s, $E_{DC-WCV} = 50$ KJ, $b = 10$ M, $D = 800$ s, $e_{\text{move}} = 8.27$ m/s, e_{RF} is 3 to 5 J/s.

Using the same network partition algorithm NT-MST, we compare the tour length of anchors for APE [21], AS-DE, AS-E [19], and DSBA [15]. APE selects anchors according to whether there are nodes in the cell. AS-E chooses anchors based on the minimum energy of k hop neighbor nodes in network. DSBA selects anchors according to number of neighbor nodes

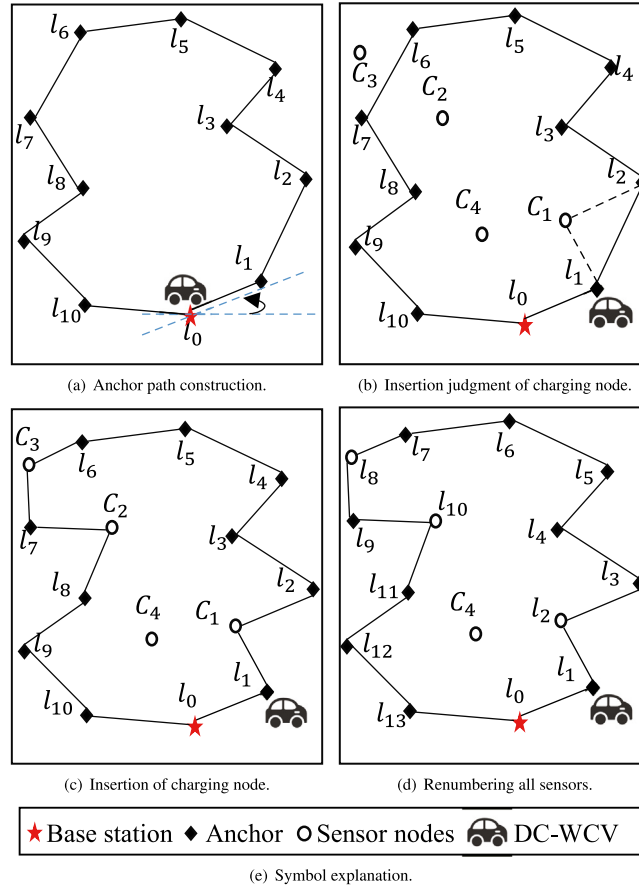


Fig. 7. Path construction process of DC-WCV.

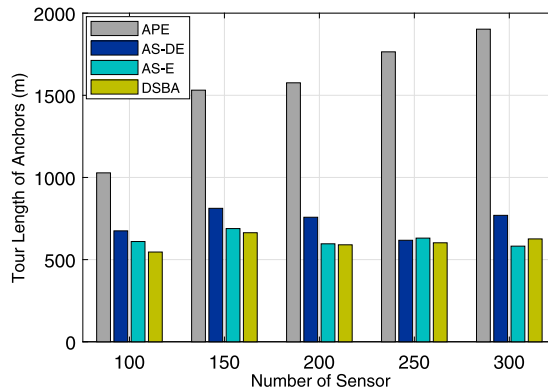


Fig. 8. Comparison of tour length of anchors.

in network. Fig. 8 shows that when the number of the sensor is the same, the tour length of APE is the longest followed by AS-DE, AS-E, and DSBA. This is because DSBA only measures sensor neighbor node number to select anchor. When nodes are distributed densely, it may need fewer anchors to cover all nodes of the network. AS-E only takes energy as the criterion to select anchor. When sensors' energy has a large gap, selected anchors may be located in a remote location. That will increase the tour length of anchors. Compared with the other two algorithms, AS-DE takes into account both the density of the sensor and the energy of neighborhood nodes. It synthetically chooses nodes with higher density and energy as anchors. Selected anchors may be remote in a dense area, resulting in longer anchors tour length. Difference from the previous three algorithms, when the sensor nodes are sparsely distributed, APE will select most of the sensor

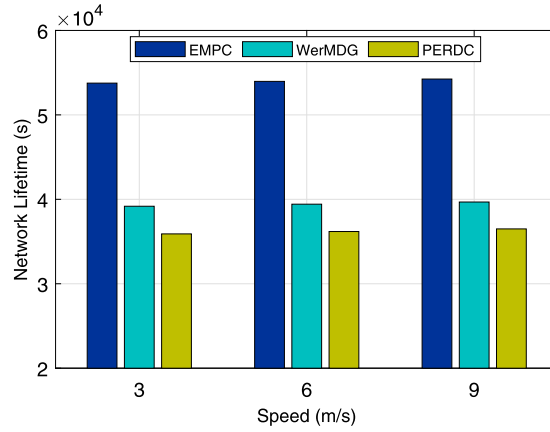


Fig. 9. Comparison of network lifetime.

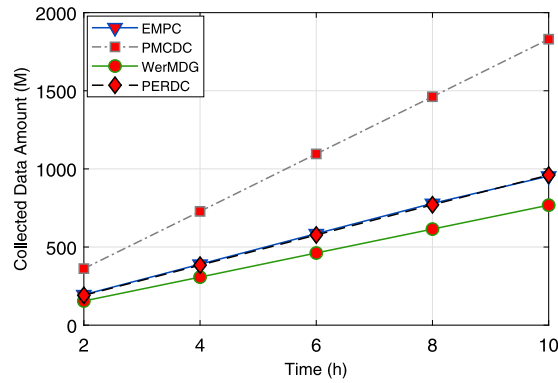


Fig. 10. Comparison of collected data amount.

nodes in the network as anchors, resulting in a long-distance to traverse all anchors. Network lifetime is measured by the time duration from network operation start to the first node running out of energy. Fig. 9 shows that the network lifetime is gradually prolonged with increasing mobile vehicle speed. This is because vehicles with higher speeds can move to sensors faster to supplement energy for sensors in time. Besides, when the mobile vehicle speed is constant, the network lifetime of EMPC is longer than that of WerMDG and PERDC. The reason is in WerMDG and PERDC, once the charging request is sent by node except anchor, the charging node has to wait to be selected as an anchor to replenish its energy. EMPC can not only supplement energy for anchor, but also charge wirelessly for charging node in a round. That makes network lifetime extend. According to the equation (17) in [21], we obtain that the maximum operating period of the PMCDC scheme is $T_{max} \approx 141$ hours, which is greater than the network lifetime of the above three schemes, indicating that the PMCDC scheme can make the current network run for a long time, even forever.

Fig. 10 shows that more and more data is collected over time. This is because network sensors are always sensing data, sending, and receiving data. Besides, the collected data amount of PMCDC algorithm is larger than that of EMPC, WerMDG, and PERDC in different periods. This is because the PMCDC scheme needs to collect data from all nodes in each tour. That makes DC-WCVs in PMCDC store more data than other schemes at the same time. Fig. 11 shows DC-WCV tour length increases with time. This is because DC-WCV in the network is in the process of moving, receiving sensing data, and supplying energy for nodes, except for supplying energy and transmitting data at the base station. DC-WCV tour length increases with time. Also, DC-WCV tour length in the EMPC algorithm is less than that in PMCDC, WerMDG, and PERDC in the same period. This is because EMPC needs to collect more data in the same period make DC-WCV stay longer, while PMCDC, WerMDG, and PERDC need less time to collect data and relatively more time to move.

As shown in Fig. 12, DC-WCV consumes more and more energy to collect data over time. This is because network sensors are perceiving data, sending, and receiving data all the time. The energy consumption of DC-WCV data collection increases with time. Also, in the same period, the energy consumption of DC-WCV data collection under PMCDC is significantly greater than that of EMPC, WerMDG, and PERDC. The energy required by DC-WCV for data collection can be measured by the collected data amount. Thus, the energy consumption of DC-WCV data collection can be obtained based on the collected data amount in Fig. 10. Fig. 13 shows that the energy consumption of DC-WCV radiofrequency

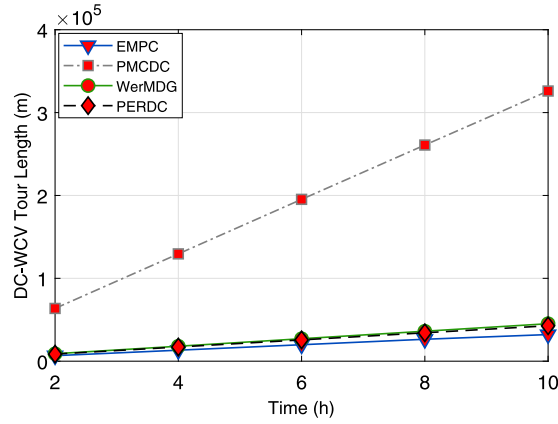


Fig. 11. Comparison of DC-WCV Tour Length.

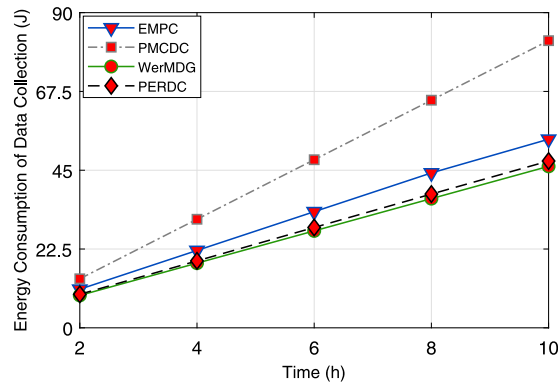


Fig. 12. Energy consumption comparison of DC-WCV data collection.

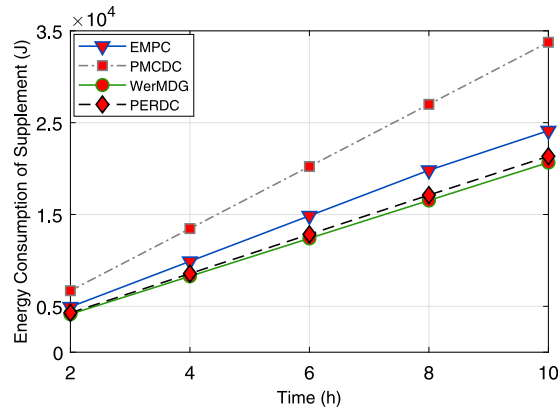


Fig. 13. Energy consumption comparison of DC-WCV radio frequency supplement.

supplement increases with time. This is because DC-WCVs are always in the process of moving, collecting data, and energy replenishment. In the same period, the energy consumption of the radiofrequency supplement under the PMCDC algorithm is significantly greater than that of EMPC, WerMDG, and PERDC. PMCDC algorithm can collect more data in the same period, so that the total residence time of DC-WCV at anchors is longer than that of EMPC, WerMDG, and PERDC. DC-WCV can provide energy for all nodes in the network in each tour. That makes DC-WCV in PMCDC can consume more energy for the radiofrequency supplement.

In this paper, the maximum value of the total residual energy of sensors is close to 5000J. As shown in Fig. 14, except for the PMCDC scheme, the total residual energy of rechargeable sensors in the network decreases gradually over time in

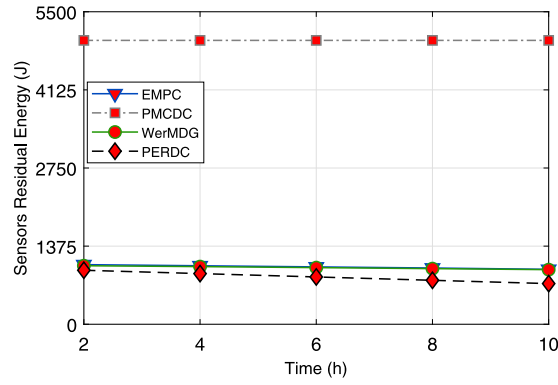


Fig. 14. Comparison of sensors residual energy.

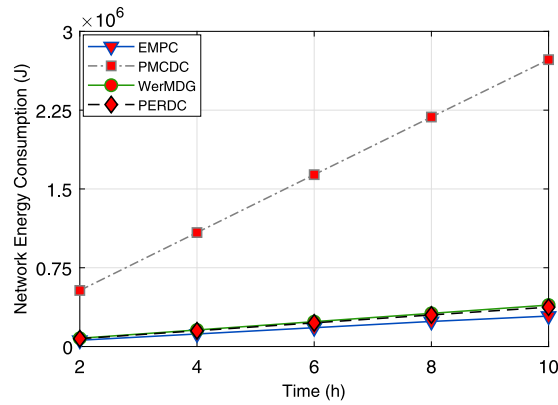


Fig. 15. Comparison of network energy consumption.

other schemes. In the same period, sensors' residual energy under the PMCDC algorithm is significantly larger than that of EMPC, WerMDG, and PERDC. PMCDC algorithm can collect more data in the same period, so that the total residence time of DC-WCV at anchors is longer than that of EMPC, WerMDG, and PERDC. DC-WCV can provide more energy for all sensors in the network, which increases the total residual energy of rechargeable sensors. That makes sensor residual energy of in PMCDC larger. Network energy consumption is the sum of energy consumption for dual-function vehicle DC-WCV and sensors. It can be obtained by the difference between initial energy and residual energy of sensor nodes, DC-WCV tour length, and energy consumption of collected data amount and radiofrequency supplement. As can be seen from Fig. 15, network energy consumption increases with time. In the same period, the network energy consumption of EMPC is less than that of PMCDC, WerMDG, and PERDC. Thus, EMPC is superior to other algorithms.

Since the DC-MCV has data collection and charging functions, the proposed scheme should consider the balance between energy consumption and data collection. That is to say, the energy consumption by collecting unit data is also the criterion to judge the performance of the proposed algorithm. The energy consumption by collecting unit data is defined as the ratio of the total energy consumption of network by the amount of data collection. The smaller the value, the better the performance of the algorithm. As shown in Fig. 16, the energy consumption by collecting unit data of the same method is similar, but different methods are different. It can be seen from Figs. 10 and 15 that EMPC collects more data than WerMDG and PERDC, but consumes less energy, which proves that EMPC has better performance. The amount of data generated by sensors is the same in the same period. EMPC and PMCDC use different collection strategies, which cause different amount of data collected. In general, the total amount of data collected by EMPC and PMCDC is similar. Different anchor selection algorithms lead to different numbers of anchors. In EMPC, a few sensor nodes with high weight are usually selected as anchors. In contrast, in PMCDC, the number of anchors selected is close to the number of sensor nodes. This makes the length of each tour in PMCDC much longer than that in EMPC. The mobile energy consumption of DC-WCV is the most important part of network energy consumption. That means the network energy consumption of PMCDC is much higher than that of EMPC. This proves that compared with PMCDC, the energy consumption of EMPC collecting unit data is lower. Therefore, the performance of EMPC is better than PMCDC in balancing energy consumption and data collection.

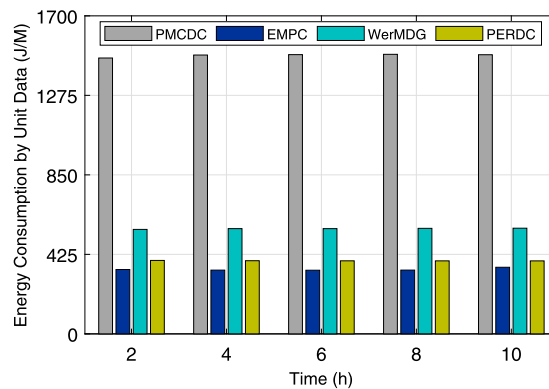


Fig. 16. Comparison of energy consumption by unit data.

6. Conclusion

This paper studies data collection and wireless charging based on the dual-function vehicle in WRSN. Under the constraints of battery energy, buffer pool size, and sensing data delay, the problem of minimizing network energy consumption is translated into DC-WCV mobile path planning problem. EMPC algorithm is proposed to solve this problem. EMPC consists of three phases: adaptive network partition, anchor selection, and path construction. Firstly, an adaptive network partitioning algorithm based on the minimum spanning tree is proposed to divide the network into several regions. In the anchor selection phase, EMPC selects anchors based on the density and energy of sensors to collect sensing data in its coverage area. Finally, EMPC designs an efficient DC-WCV moving path for anchors and charging nodes to achieve optimization object. Compared with existing algorithms WerMDG and PERDC, experimental results show that EMPC can not only effectively reduce network consumption, but also prolong network lifetime and improve collected data amount. Moreover, EMPC performs better than PMDC in balancing data collection and energy consumption.

Declaration of competing interest

The authors declare that they have no known competing financial interests or personal relationships that could have appeared to influence the work reported in this paper.

Acknowledgment

The work described in this paper was supported by the National Science Foundation of Hunan Province, China [grant number 2018JJ3692]; and the National Natural Science Foundation of China [grant number 61402542, 61772559]; and the Innovation Training Grant for Students of Central South University, China [grant number GCX2020347Y]; and the Fundamental Research Funds for the Central Universities of Central South University (China) under Grant [grant number 2020zzts592].

References

- [1] Y. Yang, C. Wang, *Wireless Rechargeable Sensor Networks*, Springer, 2015, <http://dx.doi.org/10.1007/978-3-319-17656-7>.
- [2] G. Abdul-Salaam, A.H. Abdullah, M.H. Anisi, A. Gani, A. Alelaiwi, A comparative analysis of energy conservation approaches in hybrid wireless sensor networks data collection protocols, *Telecommun. Syst.* 61 (1) (2016) 159–179, <http://dx.doi.org/10.1007/s11235-015-0092-8>.
- [3] K. Narendra, V. Varun, et al., A comparative analysis of energy-efficient routing protocols in wireless sensor networks, in: *Emerging Research in Electronics, Computer Science and Technology*, Springer, 2014, pp. 399–405, http://dx.doi.org/10.1007/978-81-322-1157-0_40.
- [4] F. Yuan, Y. Zhan, Y. Wang, Data density correlation degree clustering method for data aggregation in WSN, *IEEE Sens. J.* 14 (4) (2013) 1089–1098, <http://dx.doi.org/10.1109/JSEN.2013.2293093>.
- [5] P. Du, Q. Yang, Z. Shen, K.S. Kwak, Quality of information maximization in lifetime-constrained wireless sensor networks, *IEEE Sens. J.* 16 (19) (2016) 7278–7286, <http://dx.doi.org/10.1109/JSEN.2016.2597439>.
- [6] L. He, J. Pan, J. Xu, A progressive approach to reducing data collection latency in wireless sensor networks with mobile elements, *IEEE Trans. Mob. Comput.* 12 (7) (2012) 1308–1320, <http://dx.doi.org/10.1109/TMC.2012.105>.
- [7] T. Li, S. Tian, A. Liu, H. Liu, T. Pei, DDSV: Optimizing delay and delivery ratio for multimedia big data collection in mobile sensing vehicles, *IEEE Internet Things J.* 5 (5) (2018) 3474–3486, <http://dx.doi.org/10.1109/JIOT.2018.2847243>.
- [8] Y. Zhang, S. He, J. Chen, Near optimal data gathering in rechargeable sensor networks with a mobile sink, *IEEE Trans. Mob. Comput.* 16 (6) (2016) 1718–1729, <http://dx.doi.org/10.1109/TMC.2016.2603152>.
- [9] X.-W. Zhang, H.-P. Dai, L.-J. Xu, G.-H. Chen, Mobility-assisted data gathering strategies in WSNs, *Ruanjian Xuebao/J. Softw.* 24 (2) (2013) 198–214.
- [10] J. Wang, T. Si, X. Wu, X. Hu, Y. Yang, Sustaining a perpetual wireless sensor network by multiple on-demand mobile wireless chargers, in: 2015 IEEE 12th International Conference on Networking, Sensing and Control, IEEE, 2015, pp. 533–538, <http://dx.doi.org/10.1109/ICNSC.2015.7116093>.

- [11] C. Lin, Y. Wu, Z. Liu, M.S. Obaidat, C.W. Yu, G. Wu, GTCharge: A game theoretical collaborative charging scheme for wireless rechargeable sensor networks, *J. Syst. Softw.* 121 (2016) 88–104, <http://dx.doi.org/10.1016/j.jss.2016.08.046>.
- [12] L. He, L. Kong, Y. Gu, J. Pan, T. Zhu, Evaluating the on-demand mobile charging in wireless sensor networks, *IEEE Trans. Mob. Comput.* 14 (9) (2014) 1861–1875, <http://dx.doi.org/10.1109/TMC.2014.2368557>.
- [13] I. Farris, L. Militano, A. Iera, A. Molinaro, S.C. Spinella, Tag-based cooperative data gathering and energy recharging in wide area RFID sensor networks, *Ad Hoc Netw.* 36 (2016) 214–228, <http://dx.doi.org/10.1016/j.adhoc.2015.07.001>.
- [14] C. Wang, J. Li, F. Ye, Y. Yang, Recharging schedules for wireless sensor networks with vehicle movement costs and capacity constraints, in: 2014 Eleventh Annual IEEE International Conference on Sensing, Communication, and Networking, SECON, IEEE, 2014, pp. 468–476, <http://dx.doi.org/10.1109/SAHCN.2014.6990385>.
- [15] B.-H. Liu, N.-T. Nguyen, V.-T. Pham, Y.-X. Lin, Novel methods for energy charging and data collection in wireless rechargeable sensor networks, *Int. J. Commun. Syst.* 30 (5) (2017) e3050, <http://dx.doi.org/10.1002/dac.3050>.
- [16] M. Ghaleb, S. Subramaniam, M. Othman, Z. Zukarnain, An efficient hybrid data gathering algorithm based on multihop and mobile elements in WSNs, *Turkish J. Electr. Eng. Comput. Sci.* 25 (1) (2017) 605–621, <http://dx.doi.org/10.3906/elk-1311-7>.
- [17] H.L. Zhang, J. Liu, C. Feng, C. Pang, T. Li, J. He, Complex social network partition for balanced subnetworks, in: 2016 International Joint Conference on Neural Networks, IJCNN, IEEE, 2016, pp. 4177–4182, <http://dx.doi.org/10.1109/IJCNN.2016.7727744>.
- [18] P. Zhong, Y.-T. Li, W.-R. Liu, G.-H. Duan, Y.-W. Chen, N. Xiong, Joint mobile data collection and wireless energy transfer in wireless rechargeable sensor networks, *Sensors* 17 (8) (2017) 1881, <http://dx.doi.org/10.3390/s17081881>.
- [19] S. Guo, C. Wang, Y. Yang, Joint mobile data gathering and energy provisioning in wireless rechargeable sensor networks, *IEEE Trans. Mob. Comput.* 13 (12) (2014) 2836–2852, <http://dx.doi.org/10.1109/TMC.2014.2307332>.
- [20] Y. Wang, Y. Dong, S. Li, H. Wu, M. Cui, CRCM: A new combined data gathering and energy charging model for WRSN, *Symmetry* 10 (8) (2018) 319, <http://dx.doi.org/10.3390/sym10080319>.
- [21] Z. Lyu, Z. Wei, X. Wang, Y. Fan, C. Xia, L. Shi, A periodic multinode charging and data collection scheme with optimal traveling path in WRSNs, *IEEE Syst. J.* 14 (3) (2020) 3518–3529, <http://dx.doi.org/10.1109/JSYST.2020.2977984>.
- [22] T.D. Nguyen, S.-I. Chu, B.-H. Liu, C.-H. Chen, H.S. Dang, T. Perumal, Mobile charging and data gathering in multiple sink wireless sensor networks: How and why, in: 2017 International Conference on System Science and Engineering, ICSSE, IEEE, 2017, pp. 550–553, <http://dx.doi.org/10.1109/ICSSE.2017.8030935>.
- [23] T.D. Nguyen, S.-I. Chu, B.-H. Liu, L. Hu, Z.-H. Lai, Network under limited energy: New technique for using limited number of mobile devices for charging and collecting data, in: 2017 IEEE Wireless Power Transfer Conference, WPTC, IEEE, 2017, pp. 1–4, <http://dx.doi.org/10.1109/WPT.2017.7953818>.
- [24] N.-T. Nguyen, B.-H. Liu, V.-T. Pham, C.-Y. Huang, Network under limited mobile devices: A new technique for mobile charging scheduling with multiple sinks, *IEEE Syst. J.* 12 (3) (2016) 2186–2196, <http://dx.doi.org/10.1109/JSYST.2016.2628043>.
- [25] X. Wang, H. Dai, H. Huang, Y. Liu, G. Chen, W. Dou, Robust scheduling for wireless charger networks, in: IEEE INFOCOM 2019-IEEE Conference on Computer Communications, 2019, pp. 2323–2331.
- [26] P. Yang, T. Wu, H. Dai, X. Rao, X. Wang, P.-J. Wan, X. He, MORE: Multi-node mobile charging scheduling for deadline constraints, *ACM Trans. Sensor Netw.* 17 (1) (2020) 1–21, <http://dx.doi.org/10.1145/3410454>.
- [27] H. Teng, Y. Liu, A. Liu, N.N. Xiong, Z. Cai, T. Wang, X. Liu, A novel code data dissemination scheme for Internet of Things through mobile vehicle of smart cities, *Future Gener. Comput. Syst.* 94 (2019) 351–367, <http://dx.doi.org/10.1016/j.future.2018.11.039>.
- [28] M. Zhao, J. Li, Y. Yang, A framework of joint mobile energy replenishment and data gathering in wireless rechargeable sensor networks, *IEEE Trans. Mob. Comput.* 13 (12) (2014) 2689–2705, <http://dx.doi.org/10.1109/TMC.2014.2307335>.
- [29] Y. Liu, K.-Y. Lam, S. Han, Q. Chen, Mobile data gathering and energy harvesting in rechargeable wireless sensor networks, *Inform. Sci.* 482 (2019) 189–209, <http://dx.doi.org/10.1016/j.ins.2019.01.014>.
- [30] S. Li, L. Fu, S. He, Y. Sun, Near-optimal co-deployment of chargers and sink stations in rechargeable sensor networks, *ACM Trans. Embedded Comput. Syst.* 17 (1) (2017) 1–19, <http://dx.doi.org/10.1145/3070721>.
- [31] P. Jaillet, *Probabilistic Traveling Salesman Problems* (Ph.D. thesis), Massachusetts Institute of Technology, 1985.
- [32] C. Wang, J. Li, F. Ye, Y. Yang, A mobile data gathering framework for wireless rechargeable sensor networks with vehicle movement costs and capacity constraints, *IEEE Trans. Comput.* 65 (8) (2015) 2411–2427, <http://dx.doi.org/10.1109/TC.2015.2490060>.
- [33] W. Wen, S. Zhao, C. Shang, C.-Y. Chang, EAPC: Energy-aware path construction for data collection using mobile sink in wireless sensor networks, *IEEE Sens. J.* 18 (2) (2017) 890–901, <http://dx.doi.org/10.1109/JSEN.2017.2773119>.